Turkish Journal of Electrical Engineering & Computer Sciences

http://journals.tubitak.gov.tr/elektrik/

Research Article

Turk J Elec Eng & Comp Sci
(2018) 26: 184 – 193

doi:10.3906/elk-1705-206

Improved discrete sliding mode control strategy for pulse-width modulation rectifier

Jing CAO[1,*], **Chaonan TONG**[2]

[1]Department of Electrical & Control Engineering, North China University of Technology, Beijing, P.R. China
[2]Department of Automation & Electrical Engineering, University of Science and Technology Beijing, Beijing, P.R. China

Received: 21.05.2017 • **Accepted/Published Online:** 14.11.2017 • **Final Version:** 26.01.2018

Abstract: An improved sliding mode control utilizing repetitive control (ISMRC) is proposed for a three-phase pulse-width modulation (PWM) rectifier. The proposed controller integrates the advantages of both sliding mode control (SMC) and repetitive control (RC) by implementing a structure that embeds an RC controller into the equivalent control branch of an SMC controller. Both a simulation and an experiment are conducted to compare the proposed ISMRC controller with a conventional SMC controller. It is demonstrated that the fifth harmonic distortion of the current of the PWM rectifier system is controlled at 3.3%, the power factor is close to the unit, and the effect on the DC bus voltage is effectively restrained. Therefore, the proposed control strategy can improve both the steady-state performance and the dynamic transient response of a PWM rectifier control system effectively, as well as increase the robustness of the system to load disturbances and parametric uncertainties.

Key words: Pulse-width modulation rectifier, repetitive control, sliding mode control

1. Introduction

Three-phase pulse-width modulation (PWM) rectifiers are widely used in power system applications such as renewable energy, active filters, and uninterruptible power supply systems [1–3]. Compared to a diode rectifier, a PWM rectifier has the advantages of a bidirectional power flow, low harmonic input current distortion, an adjustable DC bus voltage, and input power factor regulation. In general, the performance of a PWM rectifier system depends primarily on the quality of the applied current control strategy [4]. A high-performance current control strategy is needed for PWM rectifiers.

Many control strategies have been applied to control the currents in PWM rectifier systems. Proportional integral (PI) control [5] is commonly used in stationary reference frames, but its use is limited by its inherent tracking error. Deadbeat control [6,7], which can minimize steady-state error effectively, is a popular choice for PWM rectifier system applications. To improve the dynamic performance, hysteresis control [8] offers extremely favorable dynamics but is sensitive to the frequency variations of a system. Some nonlinear control strategies, such as neural networks [9] and fuzzy-logic based controllers [10], have become popular, although they are difficult to implement. With the increasingly strict requirements for both steady-state performance and transient response, the design of an appropriate controller for PWM rectifier systems remains a challenge.

Surprisingly, sliding mode control has been successfully applied to this end [11,12] due to both its

*Correspondence: caojing@ncut.edu.cn

simplicity to implement and its robust performance. However, for sliding mode control, the main disadvantage of the system is that it has sensitivity to bounded matched uncertainties in part; therefore, the desired lack of dependence is not present throughout the control process. When a state trajectory falls outside the sliding mode, system states become easy for both parameter variations and external uncertainties to disturb, which affects the steady-state performance. For discrete-time sliding mode control, uncertainties may occur between sampling intervals. Therefore, it is difficult to keep the state constraint on the manifold in each subsequent sampling interval. These disadvantages affect the steady-state accuracy of the control system and limit the possible applications of SMC control. Consequently, sliding mode control system performance needs to be optimized.

Repetitive control (RC) can eliminate the steady-state tracking error [13,14], although it provides a relatively slow dynamic performance. Multiple studies have investigated a combination of SMC and RC and found that this combination can improve both the steady-state and the transient state dynamic performances of the control system. The most significant studies in this area are the following. Discrete-time sliding mode repetitive control was first proposed in [15], in which the control system successfully improved the tracking performance of an optical disk drive system. Relevant theory and possible applications were developed systematically in [16,17], which included research on the approach laws specified for nonlinear systems [18]. With respect to the combined structure, two control strategies have been applied to provide dual-loop antiinterference control for traditional control systems, including motors and PWM rectifiers [19,20]. By implementing an RC controller in series with an SMC controller [21], both the tracking accuracy and the transient response can be improved. It is common practice to embed an RC controller into part of an SMC controller [22]. However, the studies listed above aimed to study the RC controller improvements provided by such a setup, and few studies exist that analyze either the effects of the RC controller on the SMC controller or the stability of the entire closed-loop system.

Based on the discussion above, a novel intuitive combined-control structure control is proposed in this paper. An RC controller is embedded into the equivalent component of an SMC, and the assembly is referred to as an ISMRC controller. The composite control strategy ultimately achieves its purposes of enhancing the robustness of the system and optimizing its dynamic transient response. Finally, both simulation and experiment results verify the feasibility of the new composite control strategy.

2. System description and modeling

The main topology of a three-phase PWM rectifier is shown in Figure 1. Six power switches with three filters are connected to the grid. In Figure 1, e_a, e_b, and e_c are the supply voltages and i_a, i_b, and i_c denote the input currents. R_L is the equivalent resistor, and the inductance L forms the filter. u_{dc} and i_c represent the capacitor voltage and the capacitor current, respectively, and i_o is the load current.

The state of each power switch is determined by the gating signal, defined as S_k $(k = a,\ b,\ c)$. When

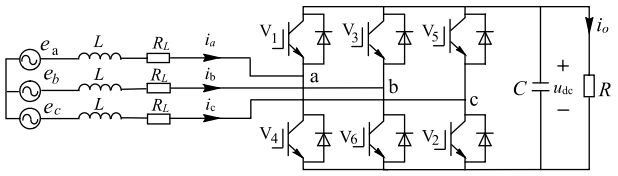

Figure 1. Standard topology of PWM rectifier.

$S_k = 1$, the switches on the upper-half bridge (V_1, V_3, and V_5) are on and those on the lower-half bridge (V_2, V_4, and V_6) are off. In contrast, when $S_k = 0$, the switches on the lower-half bridge (V_2, V_4, and V_6) are on and those on the upper-half bridge (V_1, V_3, and V_5) are off. Using the well-known Park transformation, a three-phase circuit can be transformed into a two single-phase circuit based on a rotating d-q frame, while the switch state S_k is converted to s_d, s_q. A mathematical model describing the PWM rectifier can be written in the following form [23]:

$$\frac{d}{dt}\begin{bmatrix} i_d \\ i_q \\ u_{dc} \end{bmatrix} = \begin{bmatrix} -\frac{R_L}{L} & \omega & 0 \\ -\omega & -\frac{R_L}{L} & 0 \\ 0 & 0 & -\frac{1}{CR} \end{bmatrix} \begin{bmatrix} i_d \\ i_q \\ u_{dc} \end{bmatrix} + \begin{bmatrix} -\frac{u_{dc}}{L} & 0 \\ 0 & -\frac{u_{dc}}{L} \\ \frac{i_d}{C} & \frac{i_q}{C} \end{bmatrix} \begin{bmatrix} s_d \\ s_q \end{bmatrix} + \begin{bmatrix} \frac{1}{L} & 0 \\ 0 & \frac{1}{L} \\ 0 & 0 \end{bmatrix} \begin{bmatrix} e_d \\ e_q \end{bmatrix}. \quad (1)$$

In Eq. (1), set T is the sample time. The discrete-time current model of the PWM rectifier can be obtained as

$$\begin{cases} i_d(k+1) = (1 - \frac{R_L T}{L}) i_d(k) + \omega T i_q(k) + \frac{T}{L} e_d(k) - \frac{u_{dc} T}{L} s_d(k) \\ i_q(k+1) = (1 - \frac{R_L T}{L}) i_q(k) - \omega T i_d(k) + \frac{T}{L} e_q(k) - \frac{u_{dc} T}{L} s_q(k) \end{cases}. \quad (2)$$

The discrete-time state-space model of the system can be described simply by using the following equation:

$$x(k+1) = Ax(k) + Bu(k) + Fe(k), \quad (3)$$

where $x(k) = \begin{bmatrix} i_d(k) \\ i_q(k) \end{bmatrix}$, $u(k) = \begin{bmatrix} s_d(k) \\ s_q(k) \end{bmatrix}$, $e(k) = \begin{bmatrix} e_d(k) \\ e_q(k) \end{bmatrix}$, $A = \begin{bmatrix} 1 - \frac{R_L T}{L} & \omega T \\ -\omega T & 1 - \frac{R_L T}{L} \end{bmatrix}$,

$B = \begin{bmatrix} -\frac{u_{dc} T}{L} & 0 \\ 0 & -\frac{u_{dc} T}{L} \end{bmatrix}$, and $F = \frac{T}{L}$.

An overall control diagram that is based on the system model is shown in Figure 2. In general, a conventional PWM rectifier system has a control structure comprising a dual-closed loop, such as an inner current loop and an outer voltage loop. The inner current loop regulates the input current, and the outer voltage loop adjusts the DC bus voltage. By obtaining the phase angle from the phase-locked loop (PLL), the inner current loop is decomposed into two current vector components in a synchronous rotational frame: an active vector i_d and a reactive vector i_q. When the load changes, a large fluctuation occurs in the DC bus voltage. To keep the voltage constant, a fast response is required for the active current controller tracking the reference from the outer voltage loop. The faster the current can adjust, the more stable the DC bus voltage is. Reactive current control can optimize the input power factor to a unit value. An effective current control strategy that can both eliminate the influence of the load change and maintain a unity power factor is needed. This paper primarily investigates the inner current loop; capacitor voltage control is not considered.

3. Materials and methods

3.1. Principles of conventional sliding mode control

Consider the multivariable discrete-time system in Eq. (3). The first step in designing a sliding-mode controller is selecting the sliding surface function [24]. For our current tracking system, we choose the sliding surface

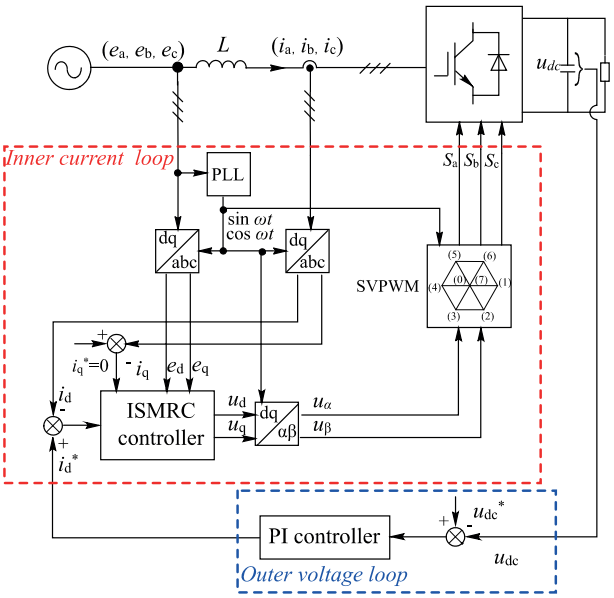

Figure 2. Control diagram of three-phase PWM rectifier.

function $\sigma(k)$ given by the following:

$$\sigma(k) = \begin{bmatrix} \sigma_d(k) \\ \sigma_q(k) \end{bmatrix} = \begin{bmatrix} c_1(i_d(k) - i_d^*(k)) \\ c_2(i_q(k) - i_q^*(k)) \end{bmatrix}, \tag{4}$$

where c_1 and c_2 are constant.

To reduce the chattering phenomenon, a reaching law based on Gao's method [25] is utilized, described as

$$\sigma(k+1) = \sigma(k) - \varepsilon T sat(\sigma(k)) - qT\sigma(k), \tag{5}$$

with the ranges of the parameters given by $0 < qT < 1$ and $\varepsilon T > 0$.

The saturation function $sat(\sigma(k))$ is adopted and defined as the following:

$$sat(\sigma(k)) = \begin{cases} +1, & \sigma(k) > \delta \\ \beta\sigma(k), & |\sigma(k)| \le \delta \\ -1, & \sigma(k) < -\delta \end{cases}, \tag{6}$$

where the ranges of the parameters are

$$\delta > 0, \quad \beta > 0, \quad \delta * \beta = 1, \quad \delta > \varepsilon T/(1 - qT).$$

To guarantee the existence of the sliding mode, the following condition needs to be satisfied:

$$\sigma(k+1) = \sigma(k) = 0. \tag{7}$$

The second step of designing a sliding mode controller is to derive a control law $u(k)$. Generally, $u(k)$ comprises two components: the equivalent control $u_{eq}(k)$ and the switching control $u_{vss}(k)$. The control law can be expressed as

$$u(k) = u_{eq}(k) + u_{vss}(k). \tag{8}$$

The equivalent control law $u_{eq}(k)$ can be derived by meeting the condition in Eq. (7) based on the model in Eq. (2) as

$$u_{eq}(k) = \begin{bmatrix} u_{deq}(k) \\ u_{qeq}(k) \end{bmatrix} = \begin{bmatrix} \frac{(R_L - \omega L) i_d(k) + e_d(k) + u^*_{re}(k)}{u_{dc}} \\ \frac{(R_L + \omega L) i_q(k) + e_q(k) + u^*_{rq}(k)}{u_{dc}} \end{bmatrix}, \tag{9}$$

where $\begin{bmatrix} u^*_{rd}(k) \\ u^*_{rq}(k) \end{bmatrix} = \begin{bmatrix} \frac{L(i^*_d(k+1) - i^*_d(k))}{T} \\ \frac{L(i^*_q(k+1) - i^*_q(k))}{T} \end{bmatrix}$.

In terms of the trajectory in the phase plane, the state trajectory of the system under the sliding mode control has two main phases known as the reaching phase and the sliding mode. The two main roles of the equivalent control are enabling the trajectory of the system into the sliding mode in a finite period of time during the reaching phase and maintaining the trajectory on the sliding surface in the sliding mode. This can be considered as the average force either pushing the trajectory of the system towards the sliding mode if it is far from the sliding surface in its initial state or maintaining a sliding behavior on the sliding surface if it is already on it in its initial state. Its switching control comes online to resist external interference once the trajectory is sliding on the switch surface. All advantages of this system, including its robustness and insensitivity to parameter variations, exist in the sliding mode but not in the reaching phase.

From a variable composition perspective, it is obvious that the control performance of the SMC depends on the accuracy of the system's dynamic model. If the parameters vary or if interference exists, the equivalent control will change and the sliding surface will drift, which seriously impacts the stability of the system. To solve this problem, repetitive control is added to the equivalent control to improve the performance of the sliding mode control. The product is referred to as the ISMRC controller.

3.2. Proposed control strategy design

For the current control that is symmetrical in d-q coordinates, we take the i_d controller as an example of current controller designation. The detailed composition of the sliding mode control is illustrated in Figure 3.

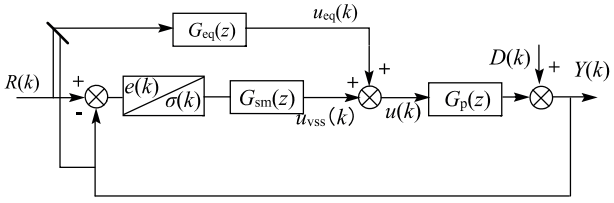

Figure 3. Control structure of conventional SMC.

In Figure 3, $G_p(z)$ represents the transfer function of the controlled object, and $D(k)$ is the uncertain interference. As mentioned above, the equivalent control is based on a system dynamic model, and the transfer function is expressed as $G_{eq}(z)$. On the other hand, the switching control branch is expressed as $G_{sm}(z)$, which includes a nonlinear saturation function from Eq. (6). As shown in Section 3.1, $G_{eq}(z)$ is based on the estimated dynamic model of the main circuit and is vulnerable to external interference during the reaching phase. For this reason, we propose a new control structure that embeds a repetitive control in the SMC controller.

RC is based on the internal model principle and is commonly employed to obtain high accuracy [14]. RC can realize zero steady-state tracking errors, especially for periodic signals. However, the dynamic response of

RC is relatively slow because of its one-cycle-delay control. The transfer function of the conventional repetitive control is [26]

$$G_{rp}(z) = \frac{K_r S(z) z^{-N+k}}{1 - Q(z) z^{-N}}, \tag{10}$$

where $Q(z)$ is a low-pass filter added to enhance the robustness of the system, $S(z)$ is selected as part of the compensation system, z^{-N} represents the cycle latency links, z^k is the phase compensation, and K_r is the control gain utilized to maintain the system stability. RC is embedded in the equivalent control branch, and the control block diagram of the composite control strategy is shown in Figure 4.

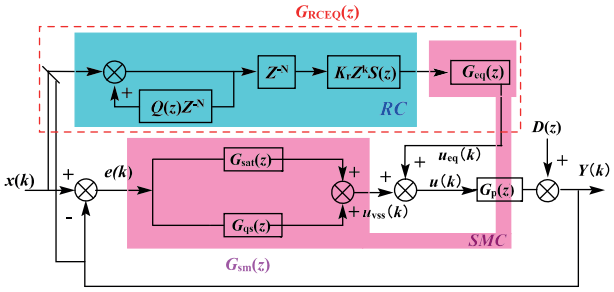

Figure 4. Control structure of ISMRC.

From Figure 4, the transfer function of the equivalent control branch $G_{RCEQ}(z)$ is defined as

$$G_{RCEQ}(z) = G_{rp}(z) \times G_{eq}(z). \tag{11}$$

The output of the ISMRC control can be expressed as

$$u(k) = R(k) G_{RCEQ}(z) + E(k) G_{sm}(z), \tag{12}$$

and $E(\mathrm{k})$ and $Y(\mathrm{k})$ are defined as

$$E(k) = R(k) - Y(k), \tag{13}$$

$$Y(k) = \left[R(k) G_{RCEQ}(z) + E(k) G_{sm}(z)\right] G_p(z) + D(k). \tag{14}$$

The equivalent control law $u_{eqN}(k)$ can be obtained as

$$u_{eqN}(k) = \begin{bmatrix} u_{deqN}(k) \\ u_{qeqN}(k) \end{bmatrix} = \begin{bmatrix} Q(z) u_{deqN}(k-N) + K_r S(z) u_{deq}(k-N) + u^*_{rdN}(k) \\ Q(z) u_{qeqN}(k-N) + K_r S(z) u_{qeq}(k-N) + u^*_{rqN}(k) \end{bmatrix}, \tag{15}$$

$$\begin{bmatrix} u^*_{rdN}(k) \\ u^*_{rqN}(k) \end{bmatrix} = \begin{bmatrix} \frac{u^*_{rd}(k) - 2u^*_{rd}(k-N)}{u_{dc}} - i^*_d(k-N) \\ \frac{u^*_{rq}(k) - 2u^*_{rq}(k-N)}{u_{dc}} - i^*_q(k-N) \end{bmatrix}. \tag{16}$$

4. Results and discussion

ISMRC control was implemented to improve the control of a PWM rectifier using MATLAB/Simulink. The parameters used are shown in the Table.

The steady-state performance simulation results under ISMRC control are shown in Figure 5. The DC bus voltage (U_{dc}) is shown in Figure 5a and a comparison of the single-phase current and the voltage (e_a /i_a)

Table. Parameters of PWM rectifier system.

Switching frequency	10 kHz
Induction (L)	0.88 mH
DC bus capacitor (C)	2000 μF
Phase voltage of AC side	220 V
DC voltage	750 V

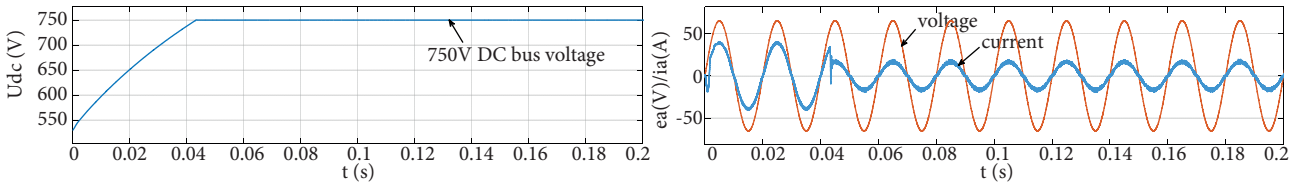

Figure 5. Steady-state performance simulation results of ISMRC controller: a) steady-state performance of DC bus voltage; b) steady-state performances of both single-phase current and voltage.

is shown in Figure 5b. At 0.045 s, the system enters the stable phase, in which the DC bus voltage is stable at 750 V (Figure 5a) and the power factor remains at unity with a stable current waveform (Figure 5a).

The total harmonic distortion (THD) results of the current are shown in Figure 6. Different control strategies obtain different THD results. For example, the THD results of the ISMRC controller (Figure 6b) are much better than those of the SMC controller (Figure 6a). It is clear that the proposed controller can reduce the THD of a current effectively.

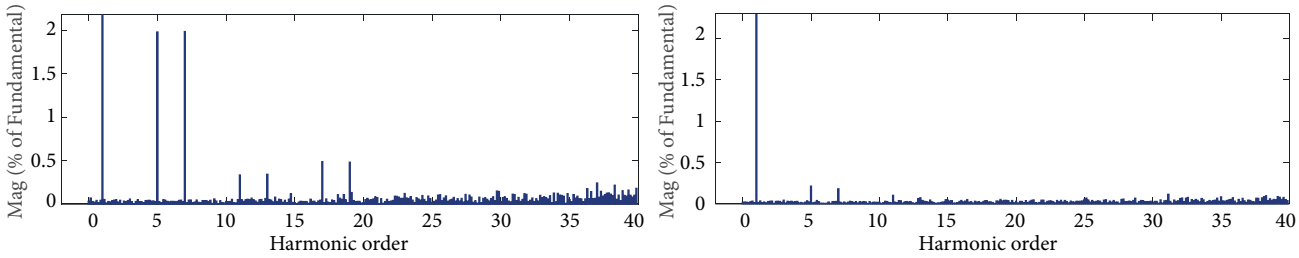

Figure 6. Different THD results using different control strategies: a) THD results of SMC; b) THD results of ISMRC.

To analyze the dynamic performance of the proposed control strategy, a simulation is conducted to compare the conventional SMC (Figure 7) with the ISMRC control (Figure 8). The external load disturbance begins at 0.2 s, the DC bus voltage (U_{dc}) (Figure 8a) is not significantly affected by the transient load mutation under ISMRC, and during the adjusting phase, ISMRC is able to maintain a smooth voltage. In contrast, the adjustability is relatively limited under SMC control. The instant that the DC bus voltage fluctuates, the current increases. A fast response is achieved by the ISMRC controller (Figure 8b), whereas an impulse current exists in the alternating process of the SMC controller (Figure 7b).

To confirm the superior performance of the proposed control strategy, experimental tests are implemented on a laboratory platform using 5 kW of power. The platform comprises both a three-phase power processing device and the main DSP (TM320F28335) control board. With the same parameters as those listed in Table, the dynamic performance of the PWM rectifier is tested, and the results are shown in Figure 9. There are two sinusoidal waveforms and one line in each figure, where the two curves (the lower) stand for the three-phase

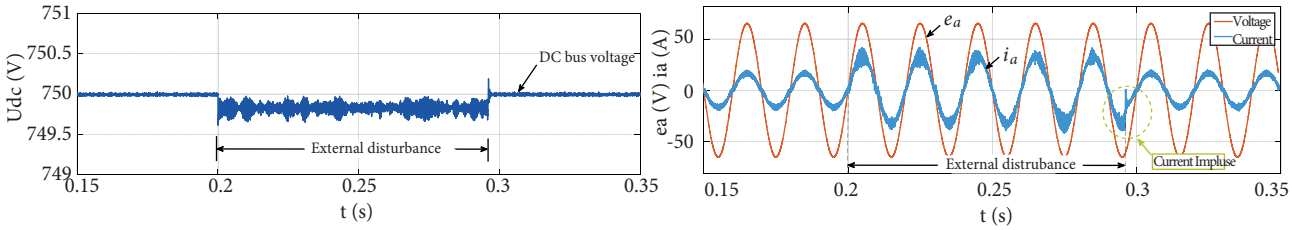

Figure 7. Dynamic simulation results of conventional SMC: a) transient response of DC bus voltage; b) transient responses of current and voltage.

current and voltage, and the line (the upper) represents the DC bus voltage. By comparing the results of the SMC control (Figure 9a) and the proposed control (Figure 9b), we can see that the proposed control strategy performs better in adjusting for the drop in the DC bus voltage. The waveform of the sinusoidal input current in Figure 9a is superior to that in Figure 9b; for instance, the inrush current and the chattering phenomenon are effectively eliminated in Figure 9b. In summary, we can conclude that under the proposed control strategy the system can achieve desirable behavior, including a well-regulated DC-bus output voltage, a low harmonic current distribution, a well-controlled power factor, and bidirectional power flow.

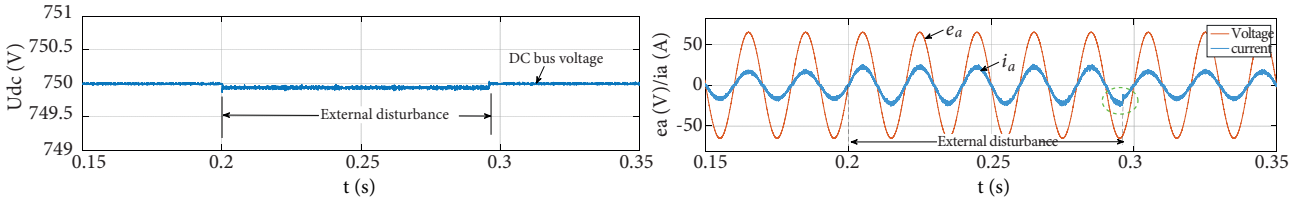

Figure 8. Dynamic simulation results of ISMRC: a) transient response of DC bus voltage; b) transient responses of current and voltage.

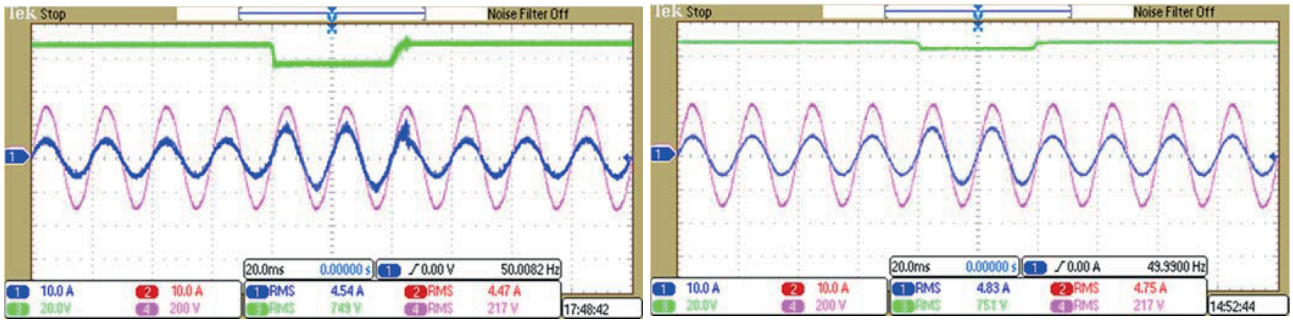

Figure 9. Experimental results of transient response: a) transient response of SMC control system; b) transient response of ISMRC control system.

5. Conclusions

In this paper, a novel ISMRC control strategy is proposed to improve the performance of a three-phase PWM rectifier system. Both the simulation and experimental results demonstrated the effectiveness and the feasibility of the proposed control strategy. Furthermore, the main conclusions are as follows: 1) The proposed controller integrates the advantages of both the SMC controller and the RC controller. By embedding the

RC controller, the robustness of the SMC controller to parametric uncertainties and external disturbances is improved effectively during the whole control process. 2) The THD results of the current obtained by the proposed control scheme are much reduced, which shows the superiority in tracking performance compared to conventional SMC control. 3) Large mutation of the DC bus voltage can be rapidly and smoothly eliminated, and the effect of the current is obviously reduced. It is shown that the proposed method improves transient state dynamic performances of the system. Due to these several advantages, the new control strategy is expected to be more attractive in applications of AC drives, renewable energy systems, and others.

References

[1] Dai J, Xu D, Wu B. A novel control scheme for current-source-converter-based PMSG wind energy conversion systems. IEEE T Power Electr 2009; 4: 963-972.

[2] Zhang Y, Qu C. Direct power control of a pulse width modulation rectifier using space vector modulation under unbalanced grid voltage. IEEE T Power Electr 2015; 30: 5892-5901.

[3] Kataoka T, Fuse Y, Nakajima D, Nishikata S. A three-phase voltage-type PWM rectifier with the function of an active power filter. In: IET 2000 Eighth International Conference on Power Electronics and Variable Speed Drives; 18–19 September 2000; London, UK. London, UK: IET. pp. 386-391.

[4] Kazmierkowski MP, Malesani L. Current control techniques for three-phase voltage-source pwm converters: a survey. IEEE T Ind Electron 1998; 45: 691-703.

[5] Dannehl J, Wessels C, Fuchs FW. Limitations of voltage-oriented PI current control of grid-connected PWM rectifiers with filters. IEEE T Ind Electron 2009; 56: 380-388.

[6] Luo A, Jin G, Xiao H. Simple control method for three-phase pulse-width modulation rectifier of switching power supply under unbalanced and distorted supply voltages. IET Power Electron 2014; 7: 2572-2581.

[7] Tiang TL, Ishak D. Modeling and simulation of deadbeat-based PI controller in a single-phase H-bridge inverter for stand-alone applications. Turk J Elec Eng & Comp Sci 2014; 22: 43-56.

[8] Dalessandro L, Drofenik U, Round SD, Kolar JW. A novel hysteresis current control for three-phase three-level PWM rectifiers. In: IEEE 2005 Applied Power Electronics Conference and Exposition; 6–10 March 2005; Austin, TX, USA. New York, NY, USA: IEEE. pp. 501-507.

[9] Pinheiro H, Jobs G, Khorasani K. Neural network-based controller for voltage PWM rectifier. In: IEEE 1996 Power Electronics Specialists Conference; 23–27 June 1996; Baveno, Italy. New York, NY, USA: IEEE. pp. 1582-1587.

[10] Bouafia A, Krim F, Gaubert JP. Fuzzy-logic-based switching state selection for direct power control of three-phase PWM rectifier. IEEE T Ind Electron 2009; 56: 1984-1992.

[11] Abdelkrim T, Berkouk EM, Benamrane K. Study and control of 5-level PWM rectifier-5-level NPC active power filter cascade using feedback control and redundant vectors. Turk J Elec Eng & Comp Sci 2012; 20: 655-677.

[12] Hamache A, Bensidhoum MO, Chekireb H. Adaptive sliding mode with time delay control based on convolutions for power reference tracking using a VSC-HVDC system. Turk J Elec Eng & Comp Sci 2017; 25: 2149-2162.

[13] Zhou K, Wang D. Digital repetitive controlled three-phase PWM rectifier. IEEE T Power Electr 2003; 18: 309-316.

[14] Li CY, Zhang DC, Zhuang XY. A survey of repetitive control. In: IEEE 2004 Proceedings of IEEE/RSJ Intelligent Robots and Systems; 28 September–2 October 2004; Sendai, Japan. New York, NY, USA: IEEE. pp. 1160-1166.

[15] Yan TH, Lin RM. Discrete-time sliding mode repetitive control for track-following of optical disk drives. In: IEEE 2002 Magnetic Recording Conference; 27–29 August 2002; Singapore. New York, NY, USA: IEEE. pp. TU-P-24-01-TU-P-24-02.

[16] Sun MX, Zhou JY, Wang YY. Discrete-time variable structure repetitive control in Industrial Technology. In: IEEE 2002 International Conference on ICIT; 11–14 December 2002; Bangkok, Thailand. New York, NY, USA: IEEE. pp. 718-723.

[17] Sun MX, Fan WY, Wang H. Discrete sliding mode repetitive control with novel reaching law. Acta Automatica Sinica 2011; 37: 1213-1221.

[18] Sun MX, Wang H, Fan WY. Discrete-time variable-structure repetitive control with power-rate reaching. Control Theory & Applications 2012; 11: 1426-1432.

[19] Lu M, Wang YG, Hu YW, Liu LH, Su N. Composite controller design for PMSM direct drive SGCMG gimbal servo system. In: IEEE 2017 Advanced Intelligent Mechatronics Conference; 3–7 July 2017; Munich, Germany. New York, NY, USA: IEEE. pp. 106-112.

[20] Cao J, Tong CN, Li HT. Hybrid dual-loop control for a three-phase PWM rectifier. In: Electrical Engineering and Automatic Control Conference; 2016; Weihai, China. Berlin, Germany: Springer Verlag. pp. 439-446.

[21] Chuei R, Cao ZW, Mitrevska M, Man ZH. Sliding mode based repetitive control for improved reference tracking. In: IEEE 2014 Proceedings of the 6th International Conference on ICMIC; 3–5 December 2014; Melbourne, Australia. New York, NY, USA: IEEE. pp. 166-171.

[22] Chen S, Lai YM, Tan SC, Tse CK. Sliding mode repetitive control of PWM voltage source inverter. In: IEEE 2007 Power Electronics and Drive Systems; 28–30 November 2007; Bangkok, Thailand. New York, NY, USA: IEEE. pp. 1069-1073.

[23] Zhang CW, Zhang X. PWM Rectifier and Its Control. Beijing, China: Mechanical Industry Press, 2003.

[24] Utkin VI. Variable structure systems with sliding modes. IEEE T Automat Contr 1977; 22: 212-222.

[25] Gao W, Wang Y, Homaifa A. Discrete-time variable structure control systems. IEEE T Ind Electron 1995; 42: 117-122.

[26] Abusara MA, Sharkh SM, Zanchetta P. Control of grid-connected inverters using adaptive repetitive and proportional resonant schemes. J Power Electron 2015; 15: 518-529.